Catalysis and Binding of Cyclophilin A with Different HIV-1 Capsid Constructs†

Daryl A. Bosco‡ and Dorothee Kern*

Department of Biochemistry, Brandeis University, Waltham, Massachusetts 02454

Received January 21, 2004; Revised Manuscript Received March 23, 2004

ABSTRACT: The prolyl isomerase cyclophilin A (CypA) is required for efficient HIV-1 replication and is incorporated into virions through a binding interaction at the Gly−Pro^{222} bond located within the capsid domain of the HIV-1 Gag precursor polyprotein (Pr^{gag}). It has recently been shown that CypA efficiently catalyzes the cis/trans isomerization of Gly−Pro^{222} within the isolated N-terminal domain of capsid (CA^{N}). To address the proposal that CypA interacts with Gly−Pro sequences in the C-terminal domain of a mature capsid, the interaction between CypA and the natively folded, full-length capsid protein (CA^{FL}) has been investigated here using nuclear magnetic resonance spectroscopy. In addition, a fragment of the Pr^{gag} protein encoding the full-matrix protein and the N-terminal domain of capsid (MA-CA^{N}) has been used to probe the catalytic interaction between CypA and an immature form of the capsid. The results discussed herein strongly suggest that Gly−Pro^{222} located within the N-terminal domain of the capsid is the preferential site for CypA binding and catalysis and that catalysis of Gly−Pro^{222} is unaffected by maturational processing at the N-terminus of the capsid.

Efficient human immunodeficiency virus type 1 (HIV-1)[1] replication requires the cellular host factor human cyclophilin A (CypA) (*1*−*3*); however, neither the precise role of CypA in HIV-1 replication nor the normal biological function of CypA is known. CypA is classified as a peptidyl prolyl isomerase (PPIase) (*4*, *5*), which is an enzyme that catalyzes the cis/trans isomerization of prolyl peptide bonds. PPIases are ubiquitous proteins, expressed in all cellular compartments and within all organisms and are represented by three distinct classes: cyclophilins, FKBPs (FK506 binding proteins), and parvulins. Since their discovery, PPIases have been implicated as folding catalysts and cellular chaperones (*6*, *7*). Recently, native state prolyl cis/trans isomerization has been proposed to modulate protein function. According to this hypothesis, cis/trans isomerization within a natively folded substrate protein induces a conformational switch that controls cellular processes involved in cell cycle regulation, cancer, and Alzheimer's disease (*8*).

During the HIV-1 replication cycle, CypA from the infected host cell is packaged into budding virions through a binding interaction within the capsid (CA) domain of the HIV-1 Gag precursor polyprotein (Pr^{gag}) (*1*, *3*). Pr^{gag} encodes the matrix (MA), CA, and nucleocapsid (NC) structural proteins and the p1, p2, and p6 peptides (Figure 1), which are liberated from Pr^{gag} by the HIV-1 protease through a process termed maturation during virion budding. MA remains associated with the virion membrane, and CA forms a conical core structure surrounding the NC/viral RNA genome complex (*9*). Proper CA core assembly and disassembly is imperative for effective release of the viral RNA genome into the host cell, and it has been suggested that CypA might be involved in CA core assembly and/or disassembly (*10*, *11*). The cryo-EM structural model of the assembled CA core predicts that the N-terminal domains of six CA molecules form an array of hexameric rings tethered to neighboring rings via dimerization through the C-terminal domain (*12*). This configuration is supported by recent hydrogen/deuterium exchange experiments in conjunction with high-resolution mass spectrometry (*13*). For unassembled CA molecules in solution, the C-terminal domain is required for dimerization (*14*, *15*) with a binding constant (K_d) of 18 ± 1 μM, which is comparable to 10 ± 3 μM for the isolated C-terminal domain (CA^{C}) (*16*). Disruption of the C-terminal domain dimer interface with the M317A (all sequence numbers refer to HIV-1 Pr^{gag}) mutation results in noninfectious virions in vivo (*16*) and aberrant CA core assembly properties in vitro (*17*). When taken together, the interactions between CA molecules mediated by the C-terminal domain are an important factor in maintaining CA core stability.

CypA specifically binds to Gly221−Pro221 (G221−P222) within an exposed flexible loop in the N-terminal domain of CA (*18*). Genetics and structural data suggest that CypA binds G221−P222 in both the context of the immature CA protein (CA encoded within Pr^{gag}) and the proteolytically

† This work was supported by NIH Grants GM62117 and GM067963 to D.K. and instrumentation grants awarded by the NSF and the Keck foundation to D.K.

* To whom correspondence should be addressed: Department of Biochemistry, MS 009, Brandeis University, 415 South Street, Waltham, MA 02454. Phone: 781-736-2354. Fax: 781-736-2316. E-mail: dkern@brandeis.edu.

‡ Current address: Department of Chemistry, The Scripps Research Institute, La Jolla, CA 92037.

[1] Abbreviations: HIV-1, human immunodeficiency virus type 1; PPIase, peptidyl prolyl *cis*-/*trans*-isomerase; CypA, cyclophilin A; Pr^{gag}, Gag precursor polyprotein; CA, full-length capsid also denoted by CA^{FL}; CA^{N}, isolated capsid N-terminal domain; CA^{C}, isolated capsid C-terminal domain; MA, matrix; MA-CA^{N}, matrix connected to capsid N-terminal domain; CsA, cyclosporin A; NMR, nuclear magnetic resonance; HSQC, heteronuclear single quantum coherence; TROSY, transverse relaxation-optimized spectroscopy; NOESY, nuclear Overhauser effect spectroscopy; TOCSY, total correlation spectroscopy; R_1, longitudinal relaxation rate.

10.1021/bi049841z CCC: $27.50
Published on Web 04/30/2004

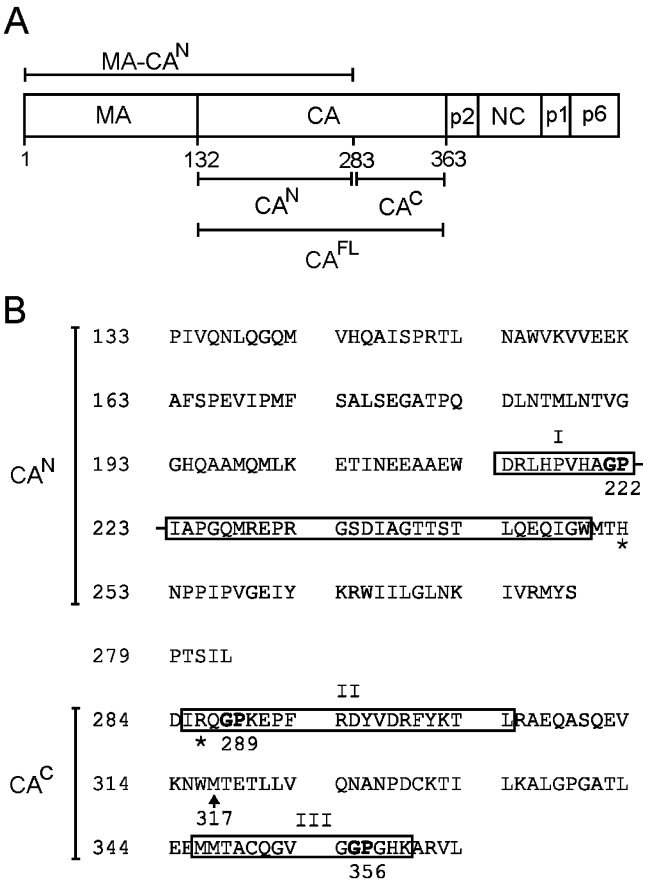

FIGURE 1: Modular structure of the HIV-1 Pr^{gag} and the amino acid sequence of the CA domain. (A) Pr^{gag} encodes the MA, CA, and NC proteins, as well as several smaller peptides (p1, p2, and p6). The constructs used in this paper are indicated CA^{FL}, CA^{N}, and MA-CA^{N}. (B) Amino acid sequence for the CA^{FL} construct used in the present paper . The three peptides (I−III) investigated in a previous peptide study are boxed (*23*), and the asterisks indicate differences in the CA^{FL} amino acid sequence from the aforementioned studies. The CypA G221−P222-binding site located within the N-terminal domain (*3*) and the proposed C-terminal domain CypA-binding sequences G288−P289 and G355−P356 (*23*) are in bold. The M317 residue at the C-terminal domain dimer interface is labeled with an arrow.

cleaved, mature CA protein. Mutagenesis of either G221 or P222 or addition of the CypA inhibitor cyclosporin A (CsA) disrupt binding of CypA to Pr^{gag} and reduce incorporation of CypA into virions, resulting in diminished HIV-1 replication and infectivity (*1*, *3*). The crystal structure of CypA bound to the isolated N-terminal domain of CA (CA^{N}), representing a mature form of CA, reveals that CypA specifically binds to G221−P222 (*18*). Furthermore, CypA was shown to catalyze the cis/trans isomerization of G221−P222 in the context of natively folded CA^{N} (*19*). However, direct investigation of the CypA interactions with the full-length CA protein containing both N- and C-terminal domains at an atomic resolution has been problematic because CA forms a complex mixture of oligomers in vitro (*20*, *21*) and the C-terminal domain in the crystal structure of CA is disordered (*22*).

Recently, CypA was reported to bind peptides derived from the C-terminal domain of CA containing the G288−P289 and G355−P356 sequences with higher affinities than a peptide derived from the N-terminal domain containing the G221−P222 sequence (Figure 1) (*23*). On the basis of this observation, the authors propose that CypA binds G221−P222 in the context of Pr^{gag} during CypA incorporation and that the process of maturation creates additional high affinity Gly−Pro-binding sites within the C-terminal domain of CA. The authors suggest that CypA may facilitate CA core disassembly by directly binding the G288−P289 and/or G355−P356 sequences and disrupting C-terminal domain dimerization. In fact, several reports suggest maturation-dependent conformational changes within CA alter the interaction between CypA and CA. Two independent groups report that CypA has a higher binding affinity for the G221−P222 sequence in the context of immature Pr^{gag} than in the context of mature CA (*24*, *25*). To date, the only structural information available for immature CA is the nuclear magnetic resonance (NMR) solution structure of the N-terminal domain of CA fused to the matrix domain (MA-CA^{N}; Figure 1), where a flexible linker connects the N terminus of CA^{N} to MA (*26*). A comparison of the isolated CA^{N} structure (*15*) with the MA-CA^{N} structure (*26*) reveals a several-angstrom shift in the CypA binding loop, which may represent a maturation-dependent conformational change that could potentially alter the CA/CypA interaction. In addition, chemical modification studies demonstrated that CypA binding at the N-terminal G221−P222 sequence in mature CA alters the accessibility of C-terminal domain cysteine residues to the fluorescein maleimide probe (*27*), an observation that offers an alternative model, where CypA binding at G221−P222 allosterically induces conformational changes in the C-terminal domain (*21*, *27*).

To directly address the question of differential CypA binding and catalysis of CA during HIV-1 maturation, the interaction between CypA and full-length CA containing both the N- and C-terminal domains (denoted by CA^{FL} for clarity) and MA-CA^{N} (Figure 1) has been investigated here using NMR spectroscopy. First, quantitative 2D ^{1}H-^{15}N heteronuclear NMR (ZZ) exchange spectroscopy (*28*, *29*) was used to measure CypA catalysis of G221−P222 within CA^{N}, CA^{FL}, and MA-CA^{N} to determine (i) whether CypA catalysis at G221−P222 is altered in the presence of the C-terminal domain, (ii) whether CypA binds and/or catalyzes additional sites within the CA C-terminal domain, and (iii) whether CypA catalysis at G221−P222 is altered when the N-terminal domain of CA is fused to the MA domain (MA-CA^{N}). Second, NMR chemical shift mapping has been employed as a direct method to further address whether CypA binds to the proposed Gly−Pro sequences (*23*) within the C-terminal domain of CA, or whether CypA binding at G221−P222 allosterically alters the conformation of the C-terminal domain. The results of these experiments reveal that CypA binding and catalysis at G221−P222 is the same in CA^{N}, CA^{FL}, and MA-CA^{N}. Furthermore, neither CypA catalysis nor direct CypA binding of the C-terminal domain Gly−Pro sequences could be detected for either CA^{FL} or the CA^{FL} M317A mutant. The results discussed herein strongly support that G221−P222 is the preferential CypA-binding site within CA. In addition, the interaction of CypA at G221−P222 within the N-terminal domain of CA is not altered when either the CA C-terminal domain or the MA domain is fused to the N-terminal domain of CA.

EXPERIMENTAL PROCEDURES

Protein Expression. Nonisotopically labeled CypA and uniformly ^{15}N-labeled CA^{N} (133−278) were expressed in BL21 (DE3) *Escherichia coli* cells and purified as described previously (*19*). The coupled chymotrypsin assay with the succinyl-Ala-Phe-Pro-Phe-*p*-nitroanilide peptide was used to assay CypA for activity as described (*30*). ^{15}N-labeled CA^{FL} (133−363) and ^{15}N-labeled MA-CA^{N} (1−283) were generous gifts from M. Summers, University of Maryland College Park. The CA^{FL} M317A plasmid was provided by W. Sundquist, University of Utah, and the CA^{FL} M317A protein was purified as described (*13*). Selective labeling of Gly residues in CA^{FL} M317A was accomplished by protein overexpression in BL21 (DE3) *E. coli* cells in M9 minimal media supplemented with 0.15 g/L 2-^{13}C,^{15}N-Gly (2-^{13}C, 99%; ^{15}N, 98% Gly purchased from Cambridge Isotope Laboratories, Inc.) and unlabeled amino acids as described (*31*). SDS−PAGE analysis was used to assess the purity of all protein preparations.

NMR Sample Preparation and Data Collection. All NMR samples were prepared in 50 mM Na_2HPO_4 at pH 6.5, 1 mM TCEP, or 1 mM dithiothreitol containing 10% D_2O, with the exception of MA-CA^{N} samples, which contained 300 mM NaCl for protein stability. The 2D ^{1}H-^{15}N heteronuclear (ZZ) exchange (*28*), transverse relaxation optimized spectroscopy (TROSY)−heteronuclear single quantum coherence (HSQC) (*32*), 3D ^{15}N-edited nuclear Overhauser effect spectroscopy (NOESY)−HSQC (100-ms mixing time), and 3D ^{15}N-edited TOCSY−HSQC (60-ms mixing time) spectra were collected either on a Varian INOVA 600 or 500 MHz spectrometer at 25 °C. NMR spectra were processed with NMRPipe (*33*) and analyzed with ANSIG (*34*). The backbone amide assignments for CA^{N} (*15*) and MA-CA^{N} (*26*) were provided by M. Summers. NMR samples for the 2D ^{1}H-^{15}N heteronuclear (ZZ) exchange spectroscopy measurements were prepared with a 12-fold excess of substrate over CypA as follows: 430 μM CA^{N}/35 μM CypA, 200 μM CA^{FL}/17 μM CypA, 200 μM CA^{N} M317A/17 μM CypA, and 560 μM MA-CA^{N}/50 μM CypA. Exchange spectra were collected with mixing times (τ_m) ranging from 0 to 800 ms. The binding interaction between unlabeled CypA and ^{15}N-labeled CA^{FL} and CA^{FL} M317A was analyzed with ^{1}H-^{15}N TROSY−HSQC spectra for samples containing 200 μM CA^{FL}/400 μM CypA and 200 μM CA^{FL} M317A/400 μM CypA, respectively.

2D ^{1}H-^{15}N Heteronuclear (ZZ) NMR Exchange Analysis. The 2D ^{1}H-^{15}N heteronuclear (ZZ) NMR exchange experiments were used to measure the rate of CypA-catalyzed cis/trans isomerization (k_{ex}) of G221−P222 within CA^{N}, CA^{FL}, and MA-CA^{N} as illustrated in Scheme 1.

Because proline residues lack a backbone amide moiety, CypA-catalyzed cis/trans isomerization of G221−P222 was measured from exchange curves for the G221 amide resonance. The low percentage of the G221$_{cis}$ auto peak and spectral overlap limited analysis of the exchange spectra to the trans auto peak and the trans exchange peak of G221 for CA^{N} and CA^{FL}, and therefore the exchange curves were fit as a function of τ_m to eqs 1a and b, which are simplified versions of previously published equations (*28*, *29*). For MA-CA^{N}, the cis exchange peak is better resolved than the trans exchange peak. Because the cis (I_{ct}) and trans (I_{tc}) exchange

Scheme 1

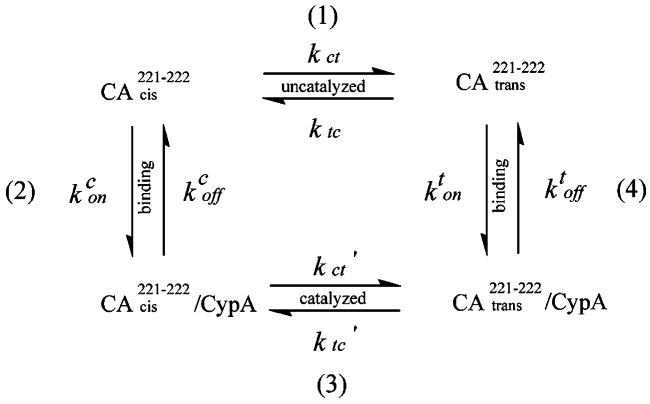

peaks have identical intensities in a 2D exchange spectrum (*35*), the intensity for the MA-CA^{N} cis exchange peak as a function of τ_m was substituted for I_{tc} in eq 1b. In eq 1a and

$$I_{tt}(\tau_m) = I_t(0)[(-(\lambda_2 - a_{11})\, e(-\lambda_1\tau_m) + (\lambda_1 - a_{11})\, e(-\lambda_2\tau_m)/(\lambda_1 - \lambda_2)] \quad (1a)$$

$$I_{tc}(\tau_m) = I_t(0)[(a_{21}\, e(-\lambda_1\tau_m) - a_{21}\, e(-\lambda_2\tau_m)/(\lambda_1 - \lambda_2)] \quad (1b)$$

b, I_{tt} is the intensity of the G221$_{trans}$ auto peak and I_{tc} is the intensity of the trans exchange peak at mixing time τ_m. $I_t(0)$ is the intensity of the trans peak at $\tau_m = 0$. $\lambda_{1,2} = {}^1/_2\{(a_{11} + a_{22}) \pm [(a_{11} - a_{22})^2 + 4k_{tc}k_{ct}]^{1/2}\}$, $a_{11} = R_{1t} + k_{tc}$, $a_{21} = -k_{tc}$, and $a_{22} = R_{1c} + k_{ct}$. R_{1c} and R_{1t} are the longitudinal relaxation rates for the cis and trans conformations of G221, respectively, which can be simplified to R_1 in the analysis because R_{1c} and R_{1t} were determined to be identical in an independent longitudinal relaxation experiment for CA^{N} (data not shown). The rate of CypA-catalyzed chemical exchange (k_{ex}) under conditions where CypA is present in substoichiometric concentrations is the sum of the individual rate constants in steps 2−4 in Scheme 1 as shown in eq 2. The populations

$$k_{ex} = (k^{c}_{on}[\mathrm{CypA}] + k_{ct}' + k^{t}_{off}) + (k^{t}_{on}[\mathrm{CypA}] + k_{tc}' + k^{c}_{off}) \quad (2)$$

of G221 in the cis and trans conformation, denoted by p_c and p_t, respectively, were determined from the relative intensities of the G221$_{trans}$ (0.86) and G221$_{cis}$ (0.14) resonances in an HSQC spectrum of CA^{N} (*15*), CA^{FL}, and MA-CA^{N} (*26*). The equilibrium constant (K_{eq}) for the cis and trans conformations is shown in eq 3. From eq 3, the individual

$$K_{eq} = p_t/p_c = k_{ct}/k_{tc} = 0.86/0.14 \quad (3)$$

rate constants k_{ct} and k_{tc} are simplified to $0.86k_{ex}$ and $0.14k_{ex}$, respectively, in eqs 1a and b. Fitting the exchange curves with eqs 1a and b results in the rate of CypA-catalyzed G221−P222 cis/trans isomerization (k_{ex}) and the longitudinal relaxation rate (R_1) for G221. Error bars for the exchange experiments were determined from the signal/noise ratio for the exchange spectra, and standard deviations were determined from the fitting procedure in Microcal Origin 6.0 professional software.

RESULTS

CypA Catalyzes G221−P222 within CA^{N}, CA^{FL}, and MA-CA^{N} with the Same Efficiency. CypA-catalyzed cis/trans

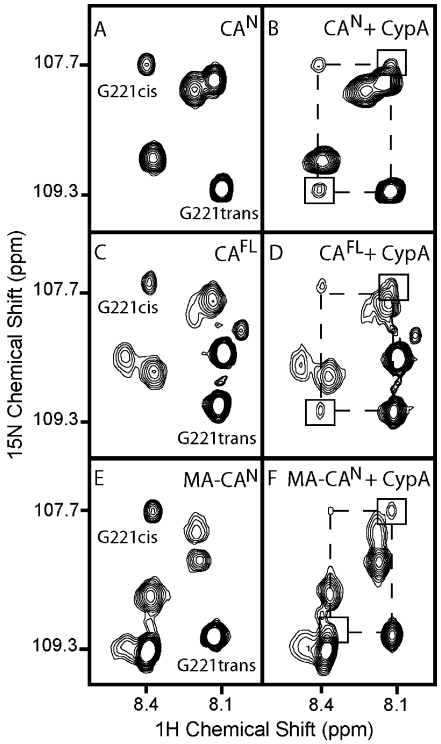

FIGURE 2: CypA catalyzes cis/trans isomerization of G221−P222 within the N-terminal domain of CA^N, CA^{FL}, and MA-CA^N. In the absence of CypA, cis/trans isomerization of G221−P222 is slow such that exchange peaks are not observed for CA^N (A), CA^{FL} (C), and MA-CA^N (E) in the 2D ^1H-^{15}N heteronuclear (ZZ) NMR exchange spectrum (*28*, *29*). Addition of substoichiometric concentrations of CypA (12:1 CA/CypA) accelerates the rate of G221−P222 cis/trans isomerization, as evidenced by the appearance of exchange peaks (boxed) corresponding to the $G221_{cis}$ and $G221_{trans}$ auto peaks in the exchange spectrum of CA^N (B), CA^{FL} (D), and MA-CA^N (F). Dashed lines connecting the exchange peaks to the $G221_{cis}$ and $G221_{trans}$ auto peaks are included for clarity. τ_m is 165 ms for all spectra (A−F).

isomerization of the G221−P222 bond within CA^N was previously detected with 2D ^1H-^{15}N heteronuclear (ZZ) exchange spectroscopy (*19*). The same technique has been employed here to investigate the enzymatic action by CypA at the G221−P222 peptide bond within differently matured forms of CA. NMR exchange spectroscopy identifies conformational exchange processes that occur with rates of chemical exchange between 0.1 and 100 s^{-1} (*36*, *37*). In the absence of CypA, cis/trans isomerization of G221−P222 is sufficiently slow ($k_{ex} < 0.1$ s^{-1}) (*38*), such that exchange peaks are not observed in the 2D exchange spectrum for CA^N, CA^{FL}, or MA-CA^N (parts A, C, and E of Figure 2). Addition of catalytic amounts of CypA accelerates G221−P222 cis/trans isomerization, resulting in exchange peaks in the 2D exchange spectrum corresponding to the $G221_{cis}$ and $G221_{trans}$ resonances for CA^N, CA^{FL}, and MA-CA^N (parts B, D, and F of Figure 2). The presence of exchange peaks provides direct evidence that CypA catalyzes G221−P222 cis/trans isomerization in CA^N, CA^{FL}, and MA-CA^N.

To quantify the catalytic efficiency for CypA catalysis of G221−P222 within CA^N, CA^{FL}, and MA-CA^N, the intensity of the exchange peaks between the $G221_{cis}$ and $G221_{trans}$ resonances and the $G221_{trans}$ auto resonance peaks were measured as a function of the mixing time (τ_m) (*28*, *29*) and fit to eqs 1a and b (see the Materials and Methods). The resulting build-up curve for the exchange peak increases as

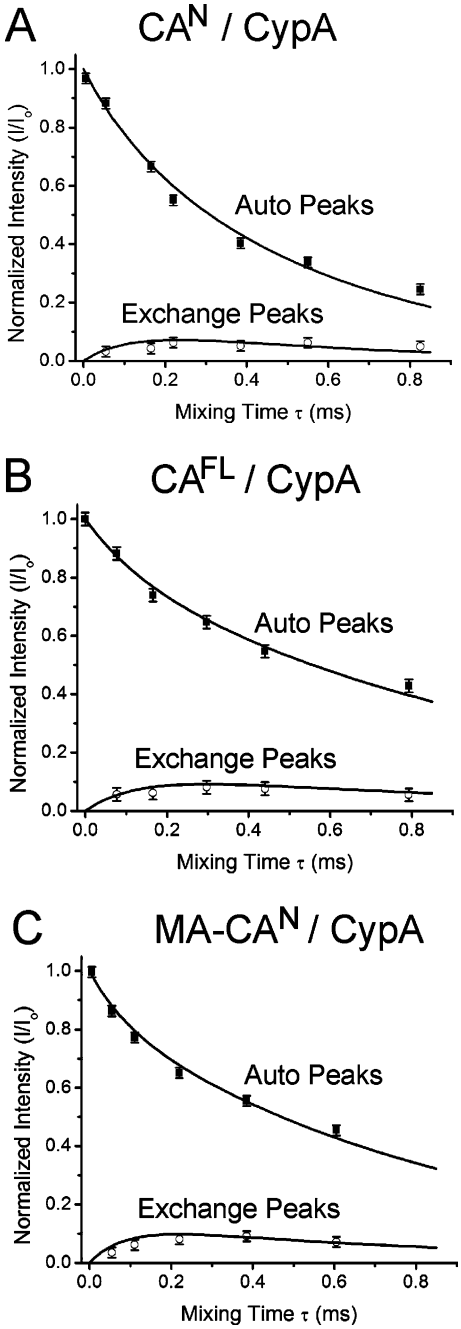

FIGURE 3: Quantification of CypA-catalyzed cis/trans isomerization (k_{ex}) of G221−P222 in CA^N (A), CA^{FL} (B), and MA-CA^N (C). Data points for the auto and exchange peaks were obtained from the normalized intensities of the respective peaks in a series of 2D ^1H-^{15}N heteronuclear (ZZ) NMR exchange spectra collected with τ_m ranging from 0 to 800 ms (A−C). The auto and exchange peaks were fitted to eqs 1a and b (*28*, *29*) (see the Materials and Methods) yielding a k_{ex} of 6.6 ± 2.4 s^{-1} for CA^N (A), 7.1 ± 1.6 s^{-1} for CA^{FL} (B), and 10.6 ± 2.5 s^{-1} for MA-CA^N (C). Results of the quantitative analysis indicate that CypA catalyzes G221−P222 within the N-terminal domain of CA^N, CA^{FL}, and MA-CA^N with similar catalytic efficiencies.

a function of τ_m because of the conformational exchange process (cis/trans isomerization) but eventually decreases because of longitudinal relaxation (R_1), whereas the autopeak exchange curve decreases biexponentially because of both the conformational exchange process and R_1 relaxation (Figure 3) (*39*). The fitting procedure results in a k_{ex} of 6.6 ± 2.4 s^{-1} and R_1 of 1.31 ± 0.09 s^{-1} for CypA-catalyzed cis/trans isomerization in CA^N (Figure 3A), where the k_{ex} is

in good agreement with a k_{ex} of 10 ± 5 s^{-1} determined previously from 3D ^{15}N-edited NOESY−HSQC spectroscopy (*19*). Quantification of CypA catalysis using 2D ^{1}H-^{15}N heteronuclear NMR (ZZ) exchange spectroscopy is advantageous over 3D ^{15}N-edited NOESY−HSQC spectroscopy in that (i) the spectral resolution is improved, (ii) the acquisition time is substantially decreased such that a series of mixing times (τ_m) can be measured, and (iii) exchange peaks corresponding to resonances with small chemical-shift differences in the ^{1}H dimension can be detected because of the absence of a diagonal. Fitting the exchange and auto peak curves for CA^{FL} resulted in a k_{ex} of 7.1 ± 1.6 s^{-1} and R_1 of 0.98 ± 0.04 s^{-1} (Figure 3B) and for MA-CA^{N} in a k_{ex} of 10.6 ± 2.5 s^{-1} and R_1 of 1.16 ± 0.06 s^{-1} (Figure 3C). The similar rate constants of exchange indicate that the maturation-dependent conformational change in the N-terminal domain of CA resulting from fusion to the MA domain (*26*) does not significantly affect the efficiency of CypA-catalyzed cis/trans isomerization of G221−P222. Furthermore, CypA catalysis at G221−P222 in the N-terminal domain is unaffected by the presence of the C-terminal domain. If maturation-dependent, high-affinity CypA-binding sites were present in the C-terminal domain, the catalytic efficiency of CypA for G221−P222 in CA^{FL} is expected to decrease because of the competitive binding and/or catalysis at these additional sites. However, the fact that CypA-catalyzed k_{ex} is similar for CA^{N} and CA^{FL} and that exchange peaks are not observed for additional Gly−Pro sequences within the C-terminal domain (Figure 4C) suggests that CypA preferentially binds and catalyzes the G221−P222 bond located in the N-terminal domain of CA.

Binding of CypA to CA^{FL}. NMR chemical shift mapping is an effective technique used to investigate protein−protein interactions (*40*) and is used here to further address the possibility that CypA binds the CA C-terminal domain directly or alters the conformation of the C-terminal domain allosterically. In a 2D ^{1}H-^{15}N TROSY−HSQC spectrum, the N-terminal domain resonances are very similar for CA^{N} and CA^{FL} (Figure 4A), indicating that the overall structure of the N-terminal domain is not significantly altered when fused to the C-terminal domain. As expected, chemical shift changes in the 2D ^{1}H-^{15}N TROSY−HSQC of CA^{N} relative to CA^{FL} are observed predominantly for residues that are near the linker region (residues 279−283) adjoining the N- and C-terminal domains (*15*) (Figures 1 and 4A). Additional amide resonances present in the CA^{FL} spectrum that are not present in the spectrum of the N-terminal domain were assigned to the C-terminal domain by process of elimination. Only 17 of the expected 75 C-terminal domain amide resonances are observable in the ^{1}H-^{15}N TROSY−HSQC spectrum (Figure 4A) because of severe line broadening. This line broadening observed for C-terminal resonances is consistent with the reversible self-association between CA molecules in solution as a consequence of intermolecular dimerization or oligomerization (*16*, *22*). In fact, the line-broadening effects for CA^{FL} are concentration-dependent (data not shown), and markedly improved spectra were obtained for NMR samples with relatively low CA^{FL} concentrations (0.20 mM; Figure 5A). The N-terminal domain resonances in CA^{FL} are not line-broadened to the same extent as the C-terminal domain resonances, presumably because the flexible linker connecting the N- and C-terminal domains enables both domains to tumble with

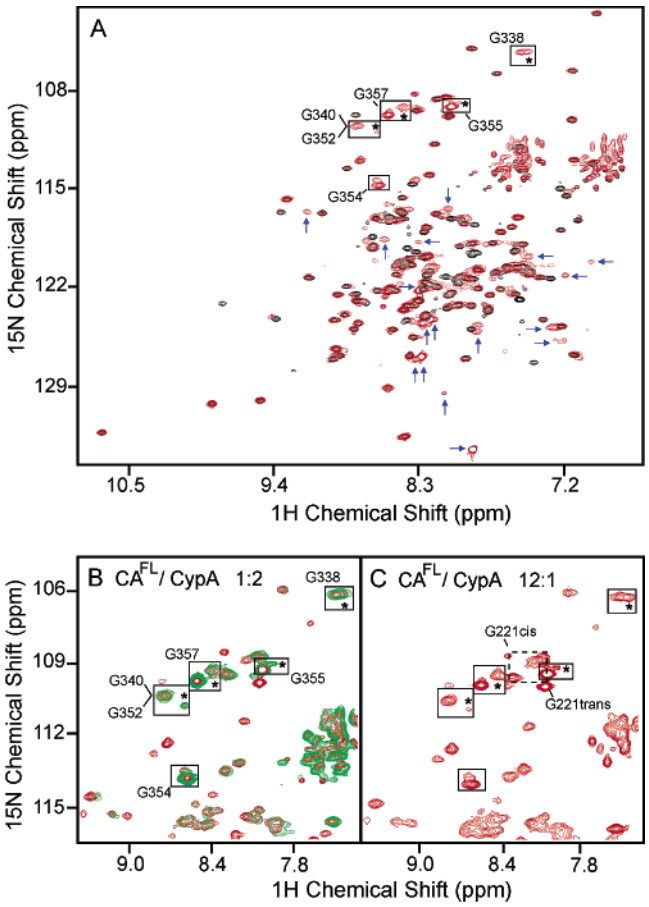

FIGURE 4: CypA binding and catalysis of CA^{FL}. (A) Comparison of the ^{1}H-^{15}N TROSY−HSQC spectrum for CA^{N} (black) with the spectrum for CA^{FL} (red) reveals that the majority of N-terminal resonances have identical chemical shifts in both spectra. All observable C-terminal domain Gly resonances are boxed and labeled with the respective sequence assignment, and duplicate resonances arising from Gly−Pro bond heterogeneity are labeled with an asterisk. Additional non-Gly C-terminal resonances observed only for CA^{FL} (red) are labeled with blue arrows. (B) Addition of 400 μM unlabeled CypA to 200 μM ^{15}N-labeled CA^{FL} (green) does not alter the chemical shifts for any of the C-terminal domain Gly resonances (labeled as described under A), as compared to the spectrum of CA^{FL} alone (red). (C) Addition of catalytic concentrations of CypA (200 μM CA^{FL}/17 μM CypA) results in exchange peaks corresponding exclusively to the $G221_{cis}$ and $G221_{trans}$ auto peaks in the 2D ^{1}H-^{15}N heteronuclear (ZZ) NMR exchange spectrum acquired with a τ_m of 165 ms (dashed lines connect exchange and auto peaks), whereas the exchange peaks are not observed for the C-terminal domain Gly resonances (labeled as described under A, except sequence assignments are omitted for clarity).

distinct rotational correlation times (τ_c), as in the case for MA-CA^{N} (*26*).

To directly address the proposed model of CypA binding to C-terminal Gly−Pro sequences (*23*), assignments were focused to the seven Gly residues within the C-terminal domain, four of which are Gly−Pro sequences (Figure 1). The 3D NMR experiments (described in detail in the next paragraph) were used to assign six of the seven C-terminal Gly resonances, which are observed in the Gly region of the CA^{FL} ^{1}H-^{15}N TROSY−HSQC spectrum but not present in the spectrum for CA^{N} (Figure 4A). Because the Gly residues are located within flexible regions of the protein (*16*), they are detected in the spectrum, whereas many other C-terminal resonances are not observable. None of the

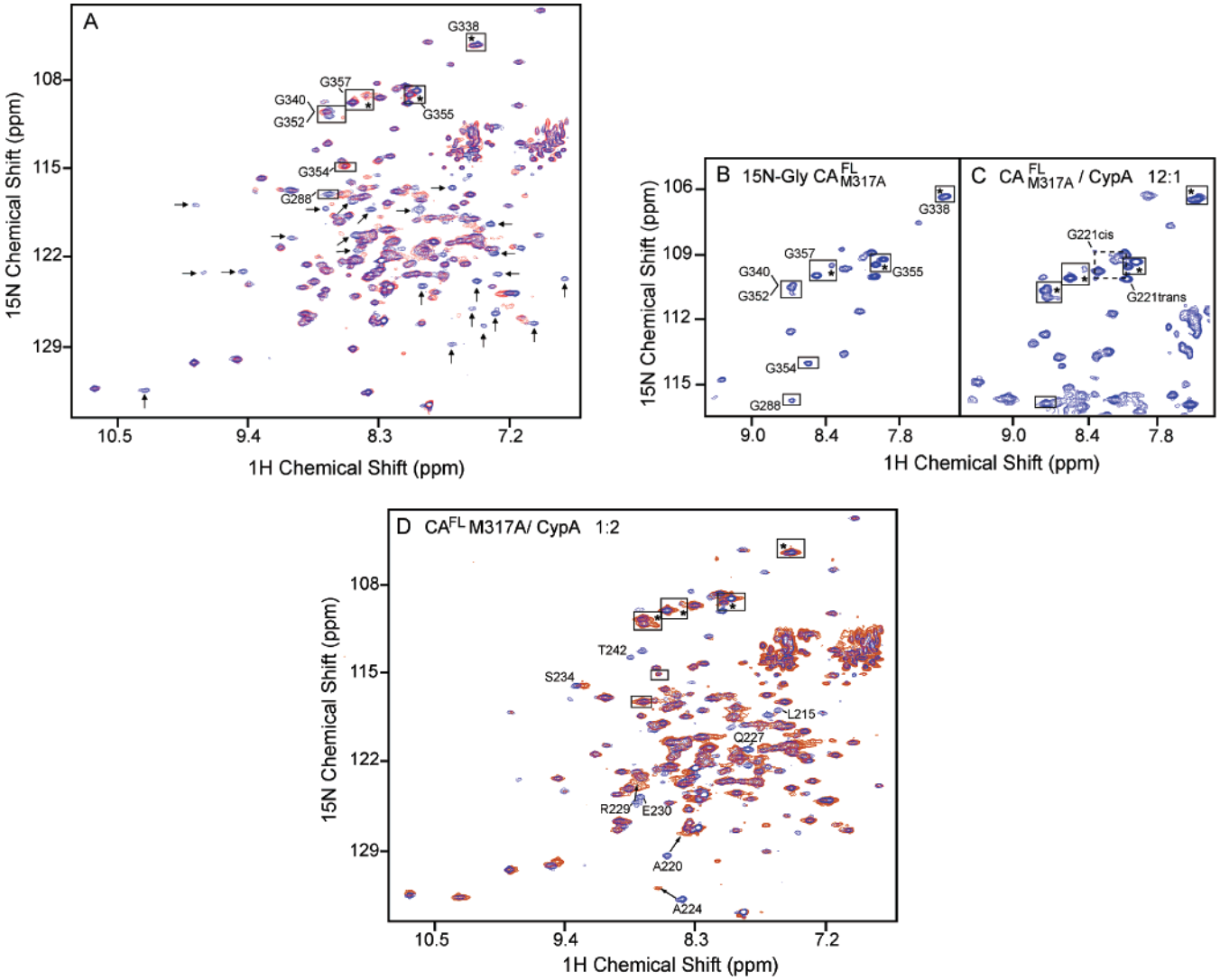

FIGURE 5: CypA binding and catalysis of the CA^{FL} M317A mutant that exhibits reduced self-association. (A) Additional resonances observed in the CA^{FL} M317A (blue) ^1H-^{15}N TROSY−HSQC spectrum resonances that are not observed for CA^{FL} WT (red) because of self-association are labeled with black arrows. All seven C-terminal domain Gly resonances are observed for CA^{FL} M317A, which are boxed and labeled with the respective sequence assignment. Duplicate resonances arising from Gly−Pro bond heterogeneity are labeled with an asterisk. (B) ^1H-^{15}N TROSY−HSQC spectrum of selectively labeled 2-^{13}C,^{15}N-Gly CA^{FL} M317A is shown with C-terminal domain Gly resonances labeled as described under A. (C) Addition of catalytic concentrations of CypA (200 μM CA^{FL} M317A/17 μM CypA) results in exchange peaks corresponding exclusively to the $G221_{cis}$ and $G221_{trans}$ auto peaks in the 2D ^1H-^{15}N heteronuclear (ZZ) NMR exchange spectrum acquired with a τ_m of 165 ms, whereas exchange peaks are not detected for the C-terminal domain Gly resonances (labeled as described under A, except sequence assignments are omitted for clarity). (D) Addition of 400 μM unlabeled CypA to 200 μM ^{15}N-labeled CA^{FL} M317A results in the chemical-shift perturbation of N-terminal domain resonances in the ^1H-^{15}N TROSY−HSQC spectrum (orange) that are expected to shift upon interaction with CypA (*19*), including the labeled residues L215, A220, A224, Q227, R229, E230, and S234 within or flanking the CypA-binding sequence in CA (*18*). Conversely, the chemical shifts for the C-terminal domain Gly resonances (boxed) are the same in the presence of excess CypA (orange) as in the absence of CypA (blue), indicating that CypA does not bind to these C-terminal domain Gly resonances.

C-terminal Gly resonances change in chemical shift in the ^{15}N TROSY−HSQC spectrum upon addition of molar excess of CypA to CA^{FL} (1:2 CA^{FL}/CypA) (Figure 4B), nor are there exchange peaks corresponding to these resonances in the 2D ^1H-^{15}N heteronuclear NMR (ZZ) exchange spectrum upon addition of catalytic concentrations of CypA (12:1 CA^{FL}/CypA) (Figure 4C), indicating that CypA does not bind or catalyze these additional C-terminal domain resonances. Conversely, addition of CypA in molar excess of CA^{FL} induces chemical shift changes for many N-terminal domain resonances, as seen previously for CA^N (*19*). The N-terminal domain resonances in CA^N were found to broaden and disappear at low concentrations of CypA and then reappear at a new chemical-shift location representing the CypA bound form (*19*), a titration pattern that is consistent with a tight-binding interaction between CypA and CA^N ($K_d = 16 \pm 4$ μM) (*14*). Similarly, at lower concentrations of CypA, N-terminal domain resonances in CA^{FL} broaden and disappear (data not shown), consistent with earlier findings that the relatively tight-binding interaction between CypA and G221−P222 is maintained for CA^{FL} (*14*, *41*).

CypA Binding and Catalysis of CA^{FL} M317A. To diminish the line broadening caused by CA^{FL} self-association, which precluded observing many of the CA^{FL} resonances in the CA^{FL}/CypA complex, the CA^{FL} M317A mutant with reduced self-association properties was investigated, allowing for a more complete analysis of the CA^{FL}/CypA complex. The point mutation M317A located at the C-terminal domain

dimer interface has been shown to disrupt dimerization in vitro and produce noninfectious HIV-1 virions in vivo (*16*).

The ^{1}H-^{15}N TROSY−HSQC spectrum for CA^{FL} M317A exhibits an overall improved spectral resolution, where ~21 additional C-terminal domain resonances are observed that are absent from the CA^{FL} WT spectrum (Figure 5A). It is noted that still only half of the expected 75 C-terminal domain amide resonances are detected, indicating that residual self-association of CA^{FL} M317A prohibits the complete alleviation of the line-broadening effects (*16*). As observed for CA^{FL} WT, line broadening for CA^{FL} M317A is concentration-dependent (data not shown), and improved spectral resolution of the CA resonances is obtained with relatively low CA^{FL} M317A concentrations (0.20 mM; Figure 5A).

The seventh C-terminal domain Gly resonance that was missing in the CA^{FL} WT spectrum could be detected in the spectrum of CA^{FL} M317A (Figure 1B), and the remaining six Gly are located at the same chemical-shift locations as in CA^{FL} WT (Figure 5A). The 3D ^{15}N-edited NOESY−HSQC and 3D ^{15}N-edited TOCSY−HSQC experiments were performed for uniformly ^{15}N-labeled and selectively labeled 2-^{13}C,^{15}N-Gly CA^{FL} M317A to sequentially assign all seven Gly resonances. In the ^{1}H-^{15}N TROSY−HSQC spectrum of 2-^{13}C,^{15}N-Gly-labeled CA^{FL} M317A (Figure 5B), all seven C-terminal domain Gly resonances are observed, as well as several N-terminal Gly and Ser resonances, where detection of Ser resonances is a general consequence of isotopic "scrambling" (*31*). All seven C-terminal domain Gly resonances have a strong nuclear Overhauser enhancement (NOE) signal at a chemical shift (4.0−4.2 ppm) corresponding to the Gly α proton in the 3D ^{15}N-edited NOESY−HSQC spectrum. In contrast, NOE patterns consistent with Ser resonances were not detected, ruling out the possibility that these signals are a result of isotopic "scrambling" of the 2-^{13}C,^{15}N-Gly label. The C-terminal sequence specific assignments shown in Figures 4 and 5 were obtained by typical inter-residual patterns to succeeding and preceding residues. For G338 and G355, the existence of a major and minor (denoted by an asterisk) conformation is most likely due to cis/trans isomerization of the G338−P339 and G355−P356 peptide bonds, respectively (Figures 4 and 5). Interestingly, the relative peak intensities of the major and minor resonances of G338 and G355 are inverted in the ^{1}H-^{15}N TROSY−HSQC spectrum for CA^{FL} WT (Figure 4) compared to that for CA^{FL} M317A (Figure 5). The low-intensity peaks near G340/G352 and G357 (denoted by an asterisk) are the putative minor conformations of G340 and G357, respectively, and are weaker in intensity in the CA^{FL} M317A spectrum (Figure 4) relative to the CA^{FL} WT spectrum (Figure 5). The altered relative intensities of the minor and major conformations of these C-terminal domain Gly resonances may reflect a shift in the cis/trans equilibrium for the respective prolyl bonds as a result of the M317A mutation and/or a result of the reduced CA^{FL} self-association. In addition, diminished self-association of CA^{FL} M317A relative to CA^{FL} WT (*16*) may explain why the G288 resonance is observed for CA^{FL} M317A but not for CA^{FL} WT (Figure 5A). Our results are in agreement with recent amide hydrogen/deuterium exchange experiments, which showed that the N- and C-terminal domains near G288 become solvent-protected upon CA^{FL} WT self-association (*13*), indicating that this region is affected by self-association.

An investigation of potential CypA-binding sites within the C-terminal domain was pursued with CA^{FL} M317A, because (i) all seven C-terminal domain Gly resonances including the proposed CypA-binding sequences G288−P289 and G355−P356 and (ii) many other C-terminal CA domain amide resonances can be observed in a ^{1}H-^{15}N TROSY−HSQC spectrum. Addition of catalytic concentrations of CypA (12:1 CA^{FL} M317A/CypA) results in exchange peaks corresponding to the G221 cis and trans resonances in a 2D ^{1}H-^{15}N heteronuclear NMR (ZZ) exchange spectrum, whereas exchange peaks for the C-terminal Gly resonances are not observed (Figure 5C). Furthermore, addition of a molar excess of CypA to CA^{FL} M317A (1:2 CA^{FL} M317A/CypA) does not induce chemical-shift changes for the C-terminal Gly resonances (Figure 5D). At lower concentrations of CypA, N-terminal domain resonances in CA^{FL} M317A broaden and disappear, indicating that the M317A mutation does not alter the tight-binding interaction between CypA and G221−P222 relative to CA^{FL} (data not shown). The overall improved spectral quality allowed for the detection of many CA^{FL} M317A amide resonances in complex with CypA (Figure 5D). Importantly, N-terminal domain resonances that are expected to shift upon interaction with CypA (*19*), including R214, L215, H216, A220, A224, Q227, R229, E230, and S234 located within or flanking the CypA-binding loop (*18*), are shifted in the ^{1}H-^{15}N TROSY−HSQC spectrum to the same chemical-shift location as CypA bound to CA^{N} (*19*) (parts A and B of Figure 6), whereas the C-terminal domain resonances are largely unaffected by CypA binding (Figures 5D and 6B). Therefore, the results obtained for CypA catalysis and binding of CA^{FL} M317A substantiate the findings for CA^{FL} WT discussed above, in that CypA preferentially binds and catalyzes the G221−P222 bond located within the N-terminal domain of CA, with no indication of an allosteric effect on the C-terminal domain. It should be noted that for the CA^{N}, CA^{FL} M317A, and MA-CA^{N} constructs studied here, the CypA-binding region within the N-terminal domain undergoes the most significant chemical-shift changes upon CypA binding and that the magnitude of these changes is similar for these constructs (Figure 6), further indicating that the interaction between CypA and the G221−P222 bond is similar for CA^{N}, CA^{FL} M317A, and MA-CA^{N}.

DISCUSSION

G221−P222 Is the Predominant CypA-Binding Site within CA. It has been proposed that the interaction between CypA and CA at G221−P222 is necessary only to incorporate CypA and that virion rearrangement during the maturation process creates additional CypA-binding sites within the C-terminal domain of CA (*23*). In support of this model, peptide studies with chymotryptic fragments of mature CA^{FL} identified two high-affinity CypA-binding sites at G288−P289 and G355−P356 within the C-terminal domain (Figure 1B) (*23*). In contrast to these indirect peptide studies, the NMR experiments reported herein permit investigation of the CypA interaction with native CA^{FL} at an atomic resolution. The fact that none of the C-terminal domain Gly resonances change in chemical shift upon addition of molar-excess concentrations of CypA is direct evidence that CypA

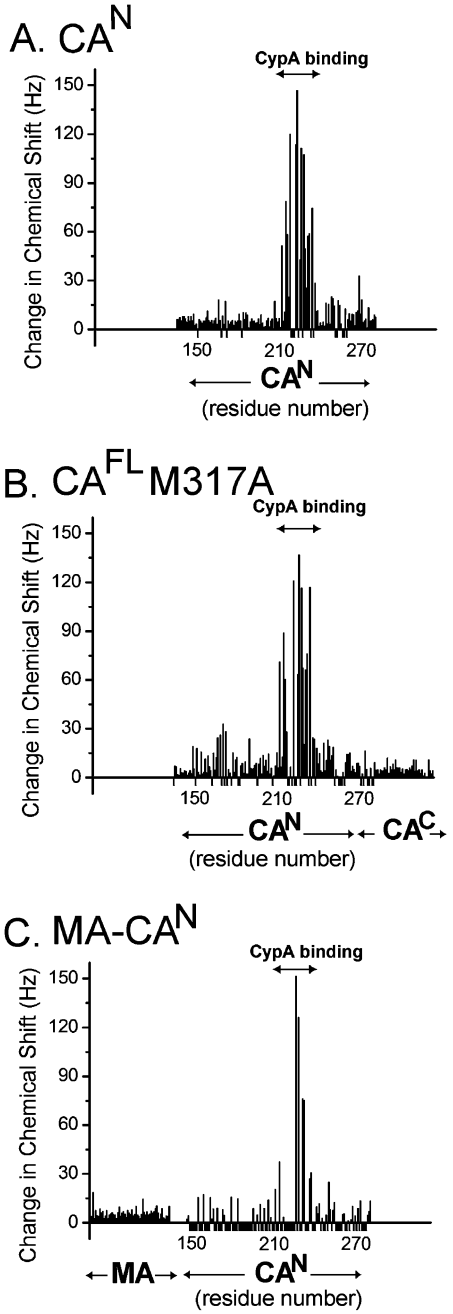

FIGURE 6: Comparison of chemical-shift changes ($[(\Delta\delta^1H)^2 + (\Delta\delta^{15}N)^2]^{1/2}$) in Hz for CA^N, CA^{FL} M317A, and MA-CA^N upon CypA binding. The CypA-binding site (residues 217−225) within CA^N is indicated, and a negative bar value is used to denote Pro residues and residues that could not be unambiguously assigned in the CypA-bound state. The largest chemical-shift changes upon CypA binding occur in the CypA-binding area in CA^N (A) as previously characterized (*19*). Location and magnitude of chemical-shift changes are almost identical upon CypA binding to CA^{FL} M317A (B) and MA-CA^N (C) with no significant chemical-shift changes for detectable CA^C resonances in CA^{FL} M317A (B) or MA resonances in MA-CA^N (C). Signal overlap and line broadening precluded the unambiguous assignment of many residues in CA^{FL} M317A and MA-CA^N. Resonances for CA^C or MA are therefore plotted with arbitrary residue numbers. Resonances belonging to MA that could be unambiguously assigned (*26*) do not change in chemical shift upon CypA binding (data not shown).

exhibits a strong preference for G221−P222 within the N-terminal domain over any Gly−Pro site within the C-terminal domain. Because the binding experiments described herein were performed with 400 μM CypA and 200 μM CA^{FL}, which represents the CypA and CA^{FL} concentrations that are ~40- and ~20-fold above the K_d for the CypA/CA-binding interaction, respectively (*14*), it is expected that an alternative C-terminal domain CypA-binding site would be detected by these experiments if it exists. Furthermore, addition of substoichiometric concentrations of CypA at a CypA/CA^{FL} ratio that is similar to what is detected in HIV-1 virions (*3*) results in CypA catalysis of the N-terminal domain G221−P222 sequence with the same efficiency as for CA^N but not for the C-terminal domain Gly−Pro sequences (Figures 4C and 5D). The conflicting results between this paper and the previous report (*23*) are most likely due to the fact that CypA binding of C-terminal sequences could only be explicitly shown for peptide fragments, whereas here the natively folded CA^{FL} protein is examined. It is not surprising that CypA binds peptides II and III in Figure 1B, because CypA exhibits broad substrate specificity for Xaa−Pro bonds, where Xaa can be any amino acid (*42*). However, the fact that the CypA-catalyzed rates of chemical exchange (k_{ex}) for native CA^N (6.6 ± 2.4 s^{-1}) and CA^{FL} (7.1 ± 1.6 s^{-1}) are the same strongly suggests that there is no competitive binding of CypA at any additional sequences within the C-terminal domain.

A second model proposes that CypA binding at G221−P222 in the N-terminal domain induces a conformational change within the C-terminal domain (*27*). In fact, there is evidence that interactions between the N- and C-terminal domains of CA^{FL} exist for assembled CA structures (*13*, *17*). The fact that only the N-terminal domain resonances shift upon addition of CypA indicates that interactions between the N- and C-terminal domains are not mediated by CypA (Figure 5C) for unassembled CA molecules, although these experiments do not rule out the possibility that CypA binding allosterically alters the C-terminal domain in the context of assembled CA-core molecules.

Is G221−P222 the functional site for CypA in HIV-1 replication? Several observations indicate that the type II turn formed by residues 224−227 within the CypA-binding sequence determine whether CypA is required for HIV-1 replication. Transfer of the HIV-1 CypA-binding sequence (217−225) into the corresponding site within the related simian immunodeficiency virus (SIVmac) vector results in CypA-dependent replication in human cells, whereas SIV normally does not require CypA for replication. Exclusion of the type II turn residues in this hybrid experiment still enables CypA incorporation but requires the CypA inhibitor cyclosporin A for viral replication (*43*). In addition, the A224E and G226D mutations within the HIV-1 capsid type II turn still allow for CypA incorporation, although this interaction is no longer required for replication (*44*, *45*). These observations indicate that residues in the immediate vicinity of G221−P222 comprise the functional site for CypA during HIV-1 replication and effectively dictate whether CypA is necessary for efficient replication.

Maturation-Dependent Alterations for CypA Binding at G221−P222. Several reports have addressed an alteration of the CypA/CA interaction as a result of maturation-induced conformational changes in CA (*24*−*27*). The recent NMR solution structure of MA-CA^N (*26*) confirmed previous predictions (*15*, *46*) that maturational refolding within the N-terminal domain involves the formation of a 13-residue β-hairpin structure that is stabilized by a salt bridge formed

between P133 at the N terminus and the side-chain carboxyl moiety of D183. Disruption of the β-hairpin structure results in noninfectious virions (*46*) that have altered CA core assembly properties (*46*, *47*), indicating that proteolytic processing and subsequent maturational refolding of the N-terminal domain are biologically relevant processes in HIV-1 replication. Comparison of the CA^N (*15*) and MA-CA^N (*26*) NMR solution structures reveals that the formation of the β hairpin is accompanied by a ~3-Å structural change in the CypA-binding loop, which may potentially affect the CypA/CA interaction. The results of the 2D ^1H-^{15}N heteronuclear NMR (ZZ) exchange experiments described herein demonstrate that CypA catalyzes cis/trans isomerization (k_{ex}) of G221−P222 in native CA^N ($6.6 \pm 2.4\ s^{-1}$) and MA-CA^N ($10.6 \pm 2.5\ s^{-1}$) with similar efficiencies, indicating that maturational refolding of the CA N-terminal domain does not significantly alter the CypA/CA interaction. These results, however, do not rule out the possibility that other maturation-dependent conformational changes in CA alter the CypA/CA interaction. The process of maturation entails proteolytic cleavage at the junction adjoining the N terminus of CA^{FL} to MA, as well as at the junction adjoining the C terminus of CA^{FL} to p2 and the NC domain (Figure 1). Studies with a truncated Pr^{gag} construct containing only CA^{FL}, p2, and NC revealed that CypA binds G221−P222 with a greater affinity when there is dimerization of the NC domain (*25*). The NC domain is largely responsible for Pr^{gag} association and oligomerization (*48*, *49*), which is thought to be important for efficient packaging of Pr^{gag} during viral assembly. Hence, it is conceivable that a stronger interaction between CypA and G221−P222 in Pr^{gag} relative to G221−P222 in immature CA facilitates CypA incorporation into virions. Additional experiments with different Pr^{gag} constructs are necessary to address how these maturation steps affect CypA binding and/or catalysis.

ACKNOWLEDGMENT

We thank Dr. Michael Summers for purified CA^{FL} and MA-CA^N and for helpful discussions pertaining to the CA^{FL} resonance assignments.

REFERENCES

1. Thali, M., Bukovsky, A., Kondo, E., Rosenwirth, B., Walsh, C. T., Sodroski, J., and Gottlinger, H. G. (1994) Functional association of cyclophilin A with HIV-1 virions, *Nature 372*, 363−365.
2. Braaten, D., and Luban, J. (2001) Cyclophilin A regulates HIV-1 infectivity, as demonstrated by gene targeting in human T cells, *EMBO J. 20*, 1300−1309.
3. Franke, E. K., Yuan, H. E., and Luban, J. (1994) Specific incorporation of cyclophilin A into HIV-1 virions, *Nature 372*, 359−362.
4. Fischer, G., Wittmann-Liebold, B., Lang, K., Kiefhaber, T., and Schmid, F. X. (1989) Cyclophilin and peptidyl-prolyl cis−trans isomerase are probably identical proteins, *Nature 337*, 476−478.
5. Takahashi, N., Hayano, T., and Suzuki, M. (1989) Peptidyl-prolyl cis−trans isomerase is the cyclosporin A-binding protein cyclophilin, *Nature 337*, 473−475.
6. Schmid, F. X. (2001) Prolyl isomerases, *Adv. Protein Chem. 59*, 243−282.
7. Gothel, S. F., and Marahiel, M. A. (1999) Peptidyl-prolyl cis−trans isomerases, a superfamily of ubiquitous folding catalysts, *Cell. Mol. Life Sci. 55*, 423−436.
8. Lu, K. P., Liou, Y. C., and Vincent, I. (2003) Proline-directed phosphorylation and isomerization in mitotic regulation and in Alzheimer's Disease, *BioEssays 25*, 174−181.
9. Turner, B. G., and Summers, M. F. (1999) Structural biology of HIV, *J. Mol. Biol. 285*, 1−32.
10. Braaten, D., Franke, E. K., and Luban, J. (1996) Cyclophilin A is required for an early step in the life cycle of human immunodeficiency virus type 1 before the initiation of reverse transcription, *J. Virol. 70*, 3551−3560.
11. Wiegers, K., Rutter, G., Schubert, U., Grattinger, M., and Krausslich, H. G. (1999) Cyclophilin A incorporation is not required for human immunodeficiency virus type 1 particle maturation and does not destabilize the mature capsid, *Virology 257*, 261−274.
12. Li, S., Hill, C. P., Sundquist, W. I., and Finch, J. T. (2000) Image reconstructions of helical assemblies of the HIV-1 CA protein, *Nature 407*, 409−413.
13. Lanman, J., Lam, T. T., Barnes, S., Sakalian, M., Emmett, M. R., Marshall, A. G., and Prevelige, P. E., Jr. (2003) Identification of novel interactions in HIV-1 capsid protein assembly by high-resolution mass spectrometry, *J. Mol. Biol. 325*, 759−772.
14. Yoo, S., Myszka, D. G., Yeh, C., McMurray, M., Hill, C. P., and Sundquist, W. I. (1997) Molecular recognition in the HIV-1 capsid/cyclophilin A complex, *J. Mol. Biol. 269*, 780−795.
15. Gitti, R. K., Lee, B. M., Walker, J., Summers, M. F., Yoo, S., and Sundquist, W. I. (1996) Structure of the amino-terminal core domain of the HIV-1 capsid protein, *Science 273*, 231−235.
16. Gamble, T. R., Yoo, S., Vajdos, F. F., von Schwedler, U. K., Worthylake, D. K., Wang, H., McCutcheon, J. P., Sundquist, W. I., and Hill, C. P. (1997) Structure of the carboxyl-terminal dimerization domain of the HIV-1 capsid protein, *Science 278*, 849−853.
17. Lanman, J., Sexton, J., Sakalian, M., and Prevelige, P. E., Jr. (2002) Kinetic analysis of the role of intersubunit interactions in human immunodeficiency virus type 1 capsid protein assembly in vitro, *J. Virol. 76*, 6900−6908.
18. Gamble, T. R., Vajdos, F. F., Yoo, S., Worthylake, D. K., Houseweart, M., Sundquist, W. I., and Hill, C. P. (1996) Crystal structure of human cyclophilin A bound to the amino-terminal domain of HIV-1 capsid, *Cell 87*, 1285−1294.
19. Bosco, D. A., Eisenmesser, E. Z., Pochapsky, S., Sundquist, W. I., and Kern, D. (2002) Catalysis of cis/trans isomerization in native HIV-1 capsid by human cyclophilin A, *Proc. Natl. Acad. Sci. U.S.A. 99*, 5247−5252.
20. Ehrlich, L. S., Agresta, B. E., and Carter, C. A. (1992) Assembly of recombinant human immunodeficiency virus type 1 capsid protein in vitro, *J. Virol. 66*, 4874−4883.
21. Agresta, B. E., and Carter, C. A. (1997) Cyclophilin A-induced alterations of human immunodeficiency virus type 1 CA protein in vitro, *J. Virol. 71*, 6921−6927.
22. Momany, C., Kovari, L. C., Prongay, A. J., Keller, W., Gitti, R. K., Lee, B. M., Gorbalenya, A. E., Tong, L., McClure, J., Ehrlich, L. S., Summers, M. F., Carter, C., and Rossmann, M. G. (1996) Crystal structure of dimeric HIV-1 capsid protein, *Nat. Struct. Biol. 3*, 763−770.
23. Endrich, M. M., Gehrig, P., and Gehring, H. (1999) Maturation-induced conformational changes of HIV-1 capsid protein and identification of two high affinity sites for cyclophilins in the C-terminal domain, *J. Biol. Chem. 274*, 5326−5332.
24. Bristow, R., Byrne, J., Squirell, J., Trencher, H., Carter, T., Rodgers, B., Saman, E., and Duncan, J. (1999) Human cyclophilin has a significantly higher affinity for HIV-1 recombinant p55 than p24, *J. Acquired Immune Defic. Syndr. 20*, 334−336.
25. Colgan, J., Yuan, H. E., Franke, E. K., and Luban, J. (1996) Binding of the human immunodeficiency virus type 1 Gag polyprotein to cyclophilin A is mediated by the central region of capsid and requires Gag dimerization, *J. Virol. 70*, 4299−4310.
26. Tang, C., Ndassa, Y., and Summers, M. F. (2002) Structure of the N-terminal 283-residue fragment of the immature HIV-1 Gag polyprotein, *Nat. Struct. Biol. 9*, 537−543.
27. Dietrich, L., Ehrlich, L. S., LaGrassa, T. J., Ebbets-Reed, D., and Carter, C. (2001) Structural consequences of cyclophilin A binding on maturational refolding in human immunodeficiency virus type 1 capsid protein, *J. Virol. 75*, 4721−4733.
28. Farrow, N. A., Zhang, O., Forman-Kay, J. D., and Kay, L. E. (1994) A heteronuclear correlation experiment for simultaneous determination of 15N longitudinal decay and chemical exchange rates of systems in slow equilibrium, *J. Biomol. NMR 4*, 727−734.
29. Tollinger, M., Skrynnikov, N. R., Mulder, F. A., Forman-Kay, J. D., and Kay, L. E. (2001) Slow dynamics in folded and unfolded states of an SH3 domain, *J. Am. Chem. Soc. 123*, 11341−11352.

30. Fischer, G., Bang, H., and Mech, C. (1984) Determination of enzymatic catalysis for the cis−trans-isomerization of peptide binding in proline-containing peptides, *Biomed. Biochim. Acta 43*, 1101−1111.
31. Waugh, D. S. (1996) Genetic tools for selective labeling of proteins with α-15N-amino acids, *J. Biomol. NMR 8*, 184−192.
32. Pervushin, K., Riek, R., Wider, G., and Wuthrich, K. (1997) Attenuated T2 relaxation by mutual cancellation of dipole−dipole coupling and chemical shift anisotropy indicates an avenue to NMR structures of very large biological macromolecules in solution, *Proc. Natl. Acad. Sci. U.S.A. 94*, 12366−12371.
33. Delaglio, F., Grzesiek, S., Vuister, G. W., Zhu, G., Pfeifer, J., and Bax, A. (1995) NMRPipe: a multidimensional spectral processing system based on UNIX pipes, *J Biomol. NMR 6*, 277−293.
34. Kraulis, P. J., Domaille, P. J., Campbell-Burk, S. L., Van Aken, T., and Laue, E. D. (1994) Solution structure and dynamics of ras p21.GDP determined by heteronuclear three- and four-dimensional NMR spectroscopy, *Biochemistry 33*, 3515−3531.
35. Willem, R. (1987) 2D NMR applied to dynamic stereochemical problems, *Prog. Nucl. Magn. Reson. Spectrosc. 20*, 1−94.
36. Macura, S., Westler, W. M., and Markley, J. L. (1994) Two-dimensional exchange spectroscopy of proteins, *Methods Enzymol. 239*, 106−144.
37. Perrin, C. L., and Dwyer, T. J. (1990) Application of Two-Dimensional NMR to Kinetics of Chemical Exchange, *Chem. Rev. 90*, 935−967.
38. Grathwohl, C., and Wuthrich, K. (1976) NMR studies of the molecular conformations in the linear oligopeptides H-(L-Ala)*n*-L-Pro-OH, *Biopolymers 15*, 2043−2057.
39. Jeener, J., Meier, B. H., Bachman, P., and Ernst, R. R. (1979) Investigation of exchange processes by two-dimensional NMR Spectroscopy, *J. Chem. Phys. 71*, 4546−4553.
40. Zuiderweg, E. R. (2002) Mapping protein−protein interactions in solution by NMR spectroscopy, *Biochemistry 41*, 1−7.
41. Grattinger, M., Hohenberg, H., Thomas, D., Wilk, T., Muller, B., and Krausslich, H. G. (1999) In vitro assembly properties of wild-type and cyclophilin-binding defective human immunodeficiency virus capsid proteins in the presence and absence of cyclophilin A, *Virology 257*, 247−260.
42. Harrison, R. K., and Stein, R. L. (1990) Substrate specificities of the peptidyl prolyl cis−trans isomerase activities of cyclophilin and FK-506 binding protein: evidence for the existence of a family of distinct enzymes, *Biochemistry 29*, 3813−3816.
43. Bukovsky, A. A., Weimann, A., Accola, M. A., and Gottlinger, H. G. (1997) Transfer of the HIV-1 cyclophilin-binding site to simian immunodeficiency virus from *Macaca mulatta* can confer both cyclosporin sensitivity and cyclosporin dependence, *Proc. Natl. Acad. Sci. U.S.A. 94*, 10943−10948.
44. Aberham, C., Weber, S., and Phares, W. (1996) Spontaneous mutations in the human immunodeficiency virus type 1 gag gene that affect viral replication in the presence of cyclosporins, *J. Virol. 70*, 3536−3544.
45. Braaten, D., Aberham, C., Franke, E. K., Yin, L., Phares, W., and Luban, J. (1996) Cyclosporine A-resistant human immunodeficiency virus type 1 mutants demonstrate that Gag encodes the functional target of cyclophilin A, *J. Virol. 70*, 5170−5176.
46. von Schwedler, U. K., Stemmler, T. L., Klishko, V. Y., Li, S., Albertine, K. H., Davis, D. R., and Sundquist, W. I. (1998) Proteolytic refolding of the HIV-1 capsid protein amino-terminus facilitates viral core assembly, *EMBO J. 17*, 1555−1568.
47. Gross, I., Hohenberg, H., Huckhagel, C., and Krausslich, H. G. (1998) N-terminal extension of human immunodeficiency virus capsid protein converts the in vitro assembly phenotype from tubular to spherical particles, *J. Virol. 72*, 4798−4810.
48. Franke, E. K., Yuan, H. E., Bossolt, K. L., Goff, S. P., and Luban, J. (1994) Specificity and sequence requirements for interactions between various retroviral Gag proteins, *J. Virol. 68*, 5300−5305.
49. Zabransky, A., Hunter, E., and Sakalian, M. (2002) Identification of a minimal HIV-1 gag domain sufficient for self-association, *Virology 294*, 141−150.

BI049841Z